

PAPER



Cite this: *Dalton Trans.*, 2015, 44, 6260

Received 8th January 2015,
Accepted 23rd February 2015

DOI: 10.1039/c5dt00075k

www.rsc.org/dalton

Efficient uptake of dimethyl sulfoxide by the desoxomolybdenum(IV) dithiolate complex containing bulky hydrophobic groups†

Yuki Hasenaka, Taka-aki Okamura* and Kiyotaka Onitsuka

A desoxomolybdenum(IV) complex containing bulky hydrophobic groups and NH...S hydrogen bonds, $(\text{Et}_4\text{N})[\text{Mo}^{\text{IV}}(\text{OSi}^t\text{BuPh}_2)(1,2\text{-S}_2\text{-3,6-}\{(4\text{-}^t\text{BuC}_6\text{H}_4)_3\text{CCONH}\}_2\text{C}_6\text{H}_2)_2]$, was synthesized. This complex promotes the oxygen-atom-transfer (OAT) reaction of DMSO by efficient uptake of the substrate into the active center. The clean OAT reaction of Me_3NO is also achieved.

Introduction

Dimethyl sulfoxide reductase (DMSOR), one of the molybdoenzymes with two unique dithiolene ligands and an alkoxo ligand, catalyzes an oxygen-atom-transfer (OAT) reaction of DMSO *via* Mo(IV) and Mo(VI) oxidation states. A molybdenum(IV) center reductively eliminates an oxygen atom from the substrates such as sulfoxides and amine *N*-oxides, resulting in the formation of a $\text{Mo}^{\text{VI}}=\text{O}$ bond (Chart 1).^{1,2}

DMSOR is involved in anaerobic respiration using dilute DMSO as an energy source in aqueous media.³ The enzyme has high affinity for DMSO with K_m values in the micromolar range.⁴ Its molecular crystal structure shows that the molybdenum site is located at the base of a large funnel-shaped depression,^{2,5} and the ligands are not exposed to the surface (Chart 1).⁶ The aromatic residues at the base of the depression provide a hydrophobic pocket to capture the methyl groups of the substrate.¹ The above results suggest the importance of the hydrophobic microenvironment for efficient uptake of the substrates.

A number of molybdenum complexes have been reported as structural and OAT reaction models.^{7–13} In particular, a siloxo-molybdenum(IV) complex with benzene-1,2-dithiolate (bdt) ligands (**7**, Chart 2) has been reported as a structural model

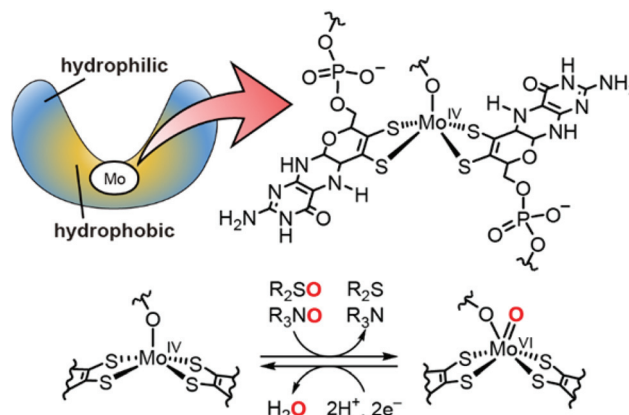


Chart 1 The structure of the active site and the catalytic cycle of dimethyl sulfoxide reductase.

for the “desoxo”-molybdenum center of DMSOR, synthesized by simple modification of the corresponding monooxomolybdenum(IV) complex.¹⁴ Moreover, a structural analogue, alkoxo-molybdenum(IV) dithiolate complex (**8**, Chart 2), has been reported to promote the OAT reaction of DMSO, a biological substrate; however, because the complex has low reactivity, excess DMSO was used.^{15,16}

The DFT calculations of the models indicated that the transient distortion of the square-pyramidal geometry that affords a vacant site *cis* to the apical ligand is important for the binding of the substrate.¹⁷ If the active center is covered with adequately bulky hydrophobic groups, and as a result, distorted by the bulkiness, then both efficient uptake of the substrate and enhancement of the reactivity to DMSO are expected to be achieved.

In our earlier studies, we have demonstrated that the introduction of four bulky CPh_3CONH substituents onto the monooxomolybdenum(IV) bdt complex resulted in a dramatic

Department of Macromolecular Science, Graduate School of Science, Osaka University, Toyonaka, Osaka 560-0043, Japan.

E-mail: tokamura@chem.sci.osaka-u.ac.jp; Fax: +81 6 6850 5474;

Tel: +81 6 6850 5451

† Electronic supplementary information (ESI) available: X-ray crystallographic data, ¹H NMR spectra of **1**, resonance Raman spectra of **1** and **3**, UV-vis spectrum of **3**, UV-vis spectral change for silylation of **4** and **5**, stability of **1** in DMF and an aqueous micellar solution, ¹H NMR spectra of the reaction mixture of **1** and DMSO, kinetic plots of the reaction of DMSO, UV-vis spectrum of molybdenum(V) species. CCDC 1041817 (1·5CH₃CN·2H₂O) and 1041818 (3·7/2CH₃CN·5/2H₂O). For ESI and crystallographic data in CIF or other electronic format see DOI: 10.1039/c5dt00075k

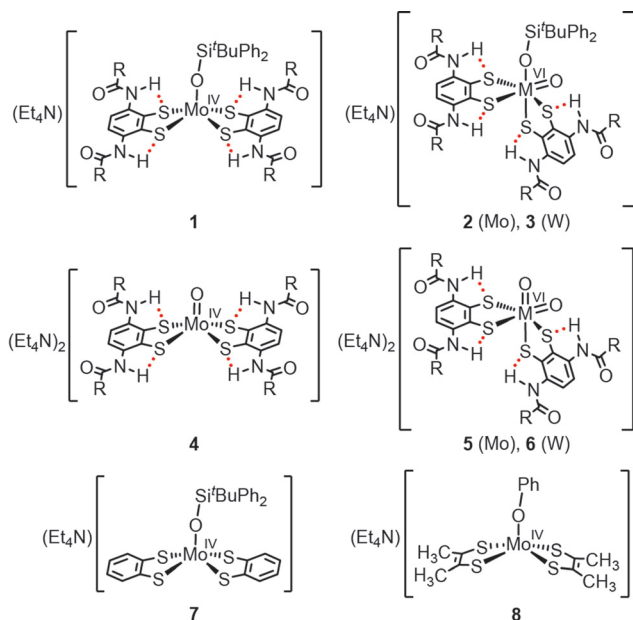
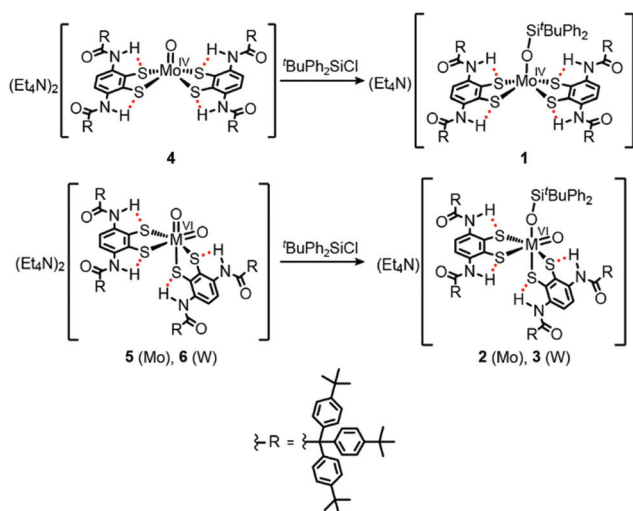


Chart 2 Designation of molybdenum and tungsten complexes (R = C(C₆H₄-4-^tBu)₃).

acceleration of the OAT reaction of Me₃NO *via* the “*cis*-attack” mechanism. This is due to the stabilization of the distorted intermediate.^{18–20}

Furthermore, we have recently reported that the monooxomolybdenum(IV) complex containing bulky hydrophobic dithiolate ligands, *i.e.* (Et₄N)₂[Mo^{IV}O(1,2-S₂-3,6- $\{(4\text{-}^t\text{BuC}_6\text{H}_4)_3\text{CCONH}\}_2\text{C}_6\text{H}_2\}_2]$ (**4**, Scheme 1), was soluble in nonpolar solvents such as toluene. The approach of a polar substrate, Me₃NO, to the active center was found to be more efficient in hydrophobic media.²¹ The hydrophobic microenvironment formed by bulky hydrophobic moieties was expected to simulate the hydrophobic pocket of DMSOR; however, **4** did not



Scheme 1 Synthesis of the complexes **1–3**.

react with DMSO owing to the strong donation of the oxo ligand to the Mo(IV) center.

Here, the synthesis and reactivity of a desoxomolybdenum(IV) complex, (Et₄N)[Mo^{IV}(OSi^tBuPh₂)(1,2-S₂-3,6- $\{(4\text{-}^t\text{BuC}_6\text{H}_4)_3\text{CCONH}\}_2\text{C}_6\text{H}_2\}_2]$ (**1**, Scheme 1), are reported. We showed that simple modification of **4** that maintains the solubility and coordination structure results in a dramatic enhancement of the reactivity of the complex to DMSO. Unlike complex **7** with unsubstituted bdt ligands, **1** promotes the OAT reaction of DMSO in both polar and nonpolar solvents, thus demonstrating the efficient uptake of DMSO in the hydrophobic microenvironment. Monooxotungsten(VI) complex **3** was also synthesized and isolated as crystals to investigate its coordination structure in the higher oxidation state.

Experimental

All procedures were performed under an argon atmosphere by the Schlenk technique. All solvents were dried and distilled under argon before use. (Et₄N)₂[Mo^{IV}O(1,2-S₂-3,6- $\{(4\text{-}^t\text{BuC}_6\text{H}_4)_3\text{CCONH}\}_2\text{C}_6\text{H}_2\}_2]$ (**4**), (Et₄N)₂[Mo^{VI}O₂(1,2-S₂-3,6- $\{(4\text{-}^t\text{BuC}_6\text{H}_4)_3\text{CCONH}\}_2\text{C}_6\text{H}_2\}_2]$ (**5**), and (Et₄N)₂[W^{VI}O₂(1,2-S₂-3,6- $\{(4\text{-}^t\text{BuC}_6\text{H}_4)_3\text{CCONH}\}_2\text{C}_6\text{H}_2\}_2]$ (**6**) were prepared by the reported method.²¹

(Et₄N)[Mo^{IV}(OSi^tBuPh₂)(1,2-S₂-3,6- $\{(4\text{-}^t\text{BuC}_6\text{H}_4)_3\text{CCONH}\}_2\text{C}_6\text{H}_2\}_2]$ (**1**)

This compound was synthesized by a modified method reported in the literature.¹⁴ To a solution of **4** (17.5 mg, 7.09 μmol) in toluene (0.7 mL) was added ^tBuPh₂SiCl (3 μL, 12 μmol), and the reaction mixture was stirred for 1 h to afford a brownish-yellow suspension. After removal of colorless precipitates by filtration, the filtrate was evaporated under reduced pressure. The resulting brownish-yellow residue was recrystallized from toluene–acetonitrile to afford light green blocks. Yield: 17.0 mg, 93%. ¹H NMR (toluene-*d*₈): δ 8.54 (s, 4H, NH), 8.10 (s, 4H, 4,5-H), 7.68 (d, *J* = 8.7 Hz, 24H, Ar), 7.41 (m, 4H, PhSi), 7.33 (d, *J* = 8.7 Hz, 24H, Ar), 7.18 (m, 2H, PhSi), 6.95 (m, 4H, PhSi), 1.36 (br, 8H, Et₄N⁺), 1.25 (s, 108H, ^tBu), 0.94 (s, 9H, ^tBuSi), 0.03 (br, 12H, Et₄N⁺). Absorption spectrum (toluene): λ_{max} (ε, M⁻¹ cm⁻¹) 363 (17 000), 420 (sh) (7300) nm. Anal. Calcd for C₁₆₄H₂₀₃N₅O₅S₄MoSi: C, 76.45; H, 7.94; N, 2.72. Found: C, 75.17; H, 7.99; N, 2.66.

As described in a previous paper, the disagreement of elemental analysis for molybdenum complexes is probably caused by their nanoporous structure in the solid state (CIF⁺).²¹ After removal of the solvent molecules from the crystals *in vacuo*, the resulting voids might be able to trap a trace amount of water even under a dry argon atmosphere. Formal addition of water to the chemical formula improved the results. The calculated values for C₁₆₄H₂₀₃N₅O₅S₄MoSi·(H₂O)_{2.5}: C, 75.13; H, 8.00; N, 2.67 are in agreement with those observed. The water molecules were also detected in ¹H NMR spectra, but the amount of water depended on the conditions.

$(\text{Et}_4\text{N})[\text{Mo}^{\text{VI}}\text{O}(\text{OSi}^t\text{BuPh}_2)(1,2\text{-S}_2\text{-3,6-}\{(4\text{-}^t\text{BuC}_6\text{H}_4)_3\text{CCONH}\}_2\text{-C}_6\text{H}_2)_2]$ (2)

This compound was not so thermodynamically stable to be isolated, therefore it was prepared *in situ* to obtain absorption spectra. To a solution of **5** (1 mM, 0.3 mL) in toluene in a 1 mm UV cell was added a $^t\text{BuPh}_2\text{SiCl}$ solution (128 mM, 4 μL) in toluene, and the cell contents were quickly mixed by shaking and allowed to stand for 8.5 h at 27 °C. The product was used for spectral measurements without further purification. Absorption spectrum (toluene): λ_{max} (ϵ , $\text{M}^{-1} \text{cm}^{-1}$) 371 (8500), 465 (sh) (5000), 583 (4900), 770 (sh) (2100) nm.

$(\text{Et}_4\text{N})[\text{W}^{\text{VI}}\text{O}(\text{OSi}^t\text{BuPh}_2)(1,2\text{-S}_2\text{-3,6-}\{(4\text{-}^t\text{BuC}_6\text{H}_4)_3\text{CCONH}\}_2\text{-C}_6\text{H}_2)_2]$ (3)

This compound was synthesized by a modified method reported in the literature.²² To a solution of **5** (30.9 mg, 12.0 μmol) in toluene (1 mL) was added $^t\text{BuPh}_2\text{SiCl}$ (5 μL , 19 μmol). The reaction mixture was stirred at r.t. for 10 min. After removal of colorless precipitates by filtration, the filtrate was evaporated. The resulting dark reddish-purple powder was recrystallized from toluene–acetonitrile to afford dark purple plates. Yield: 23.8 mg, 74%. ^1H NMR (CD_3CN): δ 7.88 (s, 4H, NH), 7.77 (s, 4H, 4,5-H), 7.63 (d, $J = 7.2$ Hz, 4H, PhSi), 7.22 (d, $J = 8.5$ Hz, 24H, Ar), 7.20 (m, 2H, PhSi), 7.16 (d, $J = 8.5$ Hz, 24H, Ar), 7.11 (dd, $J = 7.2$, 7.8 Hz, 4H, PhSi), 3.15 (q, $J = 7.2$ Hz, 8H, Et_4N^+), 1.20 (tt, $J_{\text{H-H}} = 7.2$ Hz, $J_{\text{H-N}} = 1.9$ Hz, 12H, Et_4N^+), 1.19 (s, 108H, ^tBu), 0.93 (s, 9H, $^t\text{BuSi}$). Absorption spectrum (toluene): λ_{max} (ϵ , $\text{M}^{-1} \text{cm}^{-1}$) 390 (sh) (6100), 485 (6100), 608 (sh) (2600) nm. Anal. Calcd for $\text{C}_{164}\text{H}_{203}\text{N}_5\text{O}_6\text{S}_4\text{SiW}$: C, 73.48; H, 7.63; N, 2.61. Found: C, 73.32; H, 7.51; N, 2.57.

Physical measurements

The elemental analyses were performed on a Yanaco CHN CORDER MT-5. ^1H NMR spectra were obtained with JEOL ECA-500 and ECS-400 spectrometers in toluene- d_8 and CD_3CN at 30 °C. UV-visible absorption spectra were recorded using a SHIMADZU UV-3100PC spectrometer. Infrared (IR) spectroscopic measurements were performed on a Jasco FT/IR-6100 spectrometer. Raman spectra were recorded on a Jasco NR-1800 laser Raman spectrometer with liq. N_2 cooled or a thermoelectrically cooled CCD detector. Exciting radiation was provided using an Ar^+ ion laser (514.5 nm).

Structural determination

Each single crystal of $1\cdot 5\text{CH}_3\text{CN}\cdot 2\text{H}_2\text{O}$ and $3\cdot 7/2\text{CH}_3\text{CN}\cdot 5/2\text{H}_2\text{O}$ was selected carefully and mounted on a MicroMountTM 200 μm with Nujol, which was frozen immediately in a stream of cold nitrogen at 200 K. Data collection was made on a Rigaku RAPID II Imaging Plate area detector with Mo-K α radiation (0.71075 Å) using a MicroMax-007HF microfocussing rotating anode X-ray generator and VariMax-Mo optics. The structures were solved by direct methods (SIR92²³) for $1\cdot 5\text{CH}_3\text{CN}\cdot 2\text{H}_2\text{O}$ and heavy-atom Patterson methods (PATTY²⁴) for $3\cdot 7/2\text{CH}_3\text{CN}\cdot 5/2\text{H}_2\text{O}$ and expanded Fourier techniques using SHELXL-97 or SHELXL-2014/7.²⁵ The chemical formula of **3**

contains $7/2(\text{CH}_3\text{CN})$ and $5/2(\text{H}_2\text{O})$ but the actual crystal must contain more solvents in the void. Crystallographic data are shown in Tables S1.†

Density functional theory (DFT) calculations

Geometry optimization and vibrational calculations were performed using Becke's three-parameter hybrid functionals (B3LYP) in the Gaussian 03 program package.²⁶ The basis set used for Mo and W was LanL2DZ. For other atoms (H, C, N, O, Si, S), a 6-31G** basis set was employed. The coordinates of the crystal structures, $(\text{Et}_4\text{N})[\text{Mo}^{\text{IV}}\text{O}(\text{OSi}^t\text{BuPh}_2)(\text{bdt})_2]$ ¹⁴ and $(\text{Et}_4\text{N})[\text{W}^{\text{VI}}\text{O}(\text{OSi}^t\text{BuPh}_2)(\text{bdt})_2]$,²² were used for the initial structures with some modifications.

Kinetic measurements

A reaction system containing **1** and Me_3NO was monitored spectrophotometrically in the region 280–1000 nm. The measurements were carried out in a 1 cm UV cell containing a toluene solution of **1** (0.1 mM, 3.0 mL) at 27 °C. After thermal equilibrium, a Me_3NO solution (60 mM, 10 μL) in DMF was injected through a silicone rubber cap, and the cell contents were quickly mixed by shaking. The time course of the reaction was monitored by using the absorption maximum of **2** at 583 nm. In the case in a toluene–acetonitrile solution, a solution (1 mM) of **1** in toluene–acetonitrile ($v/v = 1/1$) was treated with an acetonitrile solution of Me_3NO (60 mM, 10 μL).

The reaction between **1** and DMSO was monitored by ^1H NMR spectroscopy. A sealed-NMR tube containing **1** (1.2 mM) and DMSO (5.7 mM) in toluene- d_8 (0.6 mL) was heated at 50 °C. The measurement was carried out at 30 °C. In another case, a mixed solution of **1** (0.99 mM) and DMSO (5.4 mM) in toluene- d_8 – CD_3CN ($v/v = 1/1$) was used.

Results

Synthesis

Desoxomolybdenum(IV), monooxomolybdenum(VI), and monooxotungsten(VI) complexes, **1–3** (Chart 2), were obtained by the reactions shown in Scheme 1. First, we monitored the UV-vis spectral change of the silylation of monooxomolybdenum(IV) (**4**) and dioxomolybdenum(VI) (**5**) complexes by using a modified method reported in the literature (Fig. S1†).^{14,22} Upon adding $^t\text{BuPh}_2\text{SiCl}$ to the complexes in toluene, the absorption spectra changed with sharp isosbestic points. The silylation of complex **4** ($k_2 = 0.18 \text{ M}^{-1} \text{ s}^{-1}$) was slower than that of **5** ($k_2 = 0.29 \text{ M}^{-1} \text{ s}^{-1}$), which is probably ascribed to the weak nucleophilicity of the strongly bonded apical oxo ligand.^{17,27} On completion of silylation of **4**, we found that the UV-vis spectrum was identical to that of isolated **1**. Therefore, we regarded the spectrum of quantitatively silylated complex **5** as that of **2**. Tungsten analogue **3** was obtained by a similar method. All the complexes were soluble in nonpolar solvents such as toluene, and pure **1** and **3** were isolated as light green and dark purple blocks in 93% and 74% yields, respectively.

Molecular structures in the crystals

The molecular structures of **1** and **3** were determined by X-ray analysis. These complexes were apparently recrystallized easily, but their crystallinity was very poor. The result was similar to that observed in the case of **4**, **5**, and **6**, as previously described.²¹ Here, we mainly discuss the geometry of the metal center.

The molecular structure of **1**·5CH₃CN·2H₂O is shown in Fig. 1a. The C(C₆H₄-4-^tBu)₃ (CAR₃) moieties are bulky enough to interlock with each other in the crystal and to create walls similar to those of complex **4** that have been previously reported.²¹ The resulting hydrophobic microspace was retained both before and after silylation. The square pyramidal geometry and the linearity of Mo–O–Si (164°) were similar to those of the related siloxomolybdenum(IV) complexes (164–175°).^{14,19} All the amide NH moieties were directed toward the sulfur atoms of the dithiolate ligand, indicating the presence of NH...S hydrogen bonds.

The W center of **3**·7/2CH₃CN·5/2H₂O shows a slightly distorted octahedral geometry, which is similar to that of **6** rather than that of a monooxotungsten(VI) complex with bdt ligands (Fig. 1b).^{21,22} The bulky substituents and hydrogen bonds probably maintain the coordination structure. All the four W–S bonds in **3** were different, and the order of the bond length was W–S1 > W–S3 > W–S4 > W–S2. As described in a previous paper on complex **6**, a strong *trans* influence of the oxo ligand makes W–S1 *trans* to W=O, leading to the most anionic thiolate and the strongest (red) N1H1...S1 hydrogen bond.²¹ The

moderate (blue) and weak (green) hydrogen bonds were formed at S3 and S2 owing to the medium and weak *trans* influences of the siloxo and thiolate ligands, respectively. The other amide N4H4 is directed toward the benzene ring of the neighboring R4 moiety, probably owing to the packing in the crystal.

¹H NMR studies

Desoxomolybdenum(IV) complex **1** exhibited well-defined ¹H NMR signals in toluene-*d*₈ (Fig. S2†), which indicated that the four acylamino groups are magnetically equivalent. In the ¹H NMR spectrum of monooxotungsten(VI) complex **3**, a single set of broad signals in a polar solvent, CD₃CN, and a couple of broad signals were observed in toluene-*d*₈ (Fig. 2). The separation and broadening of signals are ascribed to the conformational change through the Bailar twist, as described for *cis*-dioxotungsten(VI) complex **5** in a previous paper.²¹ As expected, the signals in toluene-*d*₈ became sharp upon cooling to –45 °C. The partial assignment using ROESY and COSY techniques showed that the four acylamino groups are nonequivalent like in the crystal. The singlet signal at the lowest field (red a) was reasonably assigned to the amide NH proton *trans* to the oxo ligand, as observed in **6**.²¹ The protons in the other dithiolate ligand (blue and pink) were unassignable because of

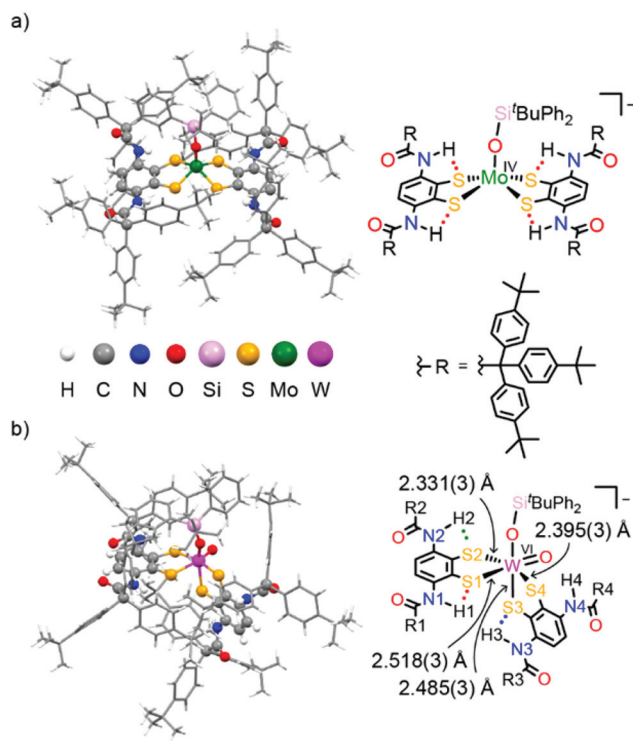


Fig. 1 Ball-and-stick models (left) and schematic drawings (right) of the anion part of (a) **1**·5CH₃CN·2H₂O and (b) **3**·7/2CH₃CN·5/2H₂O.

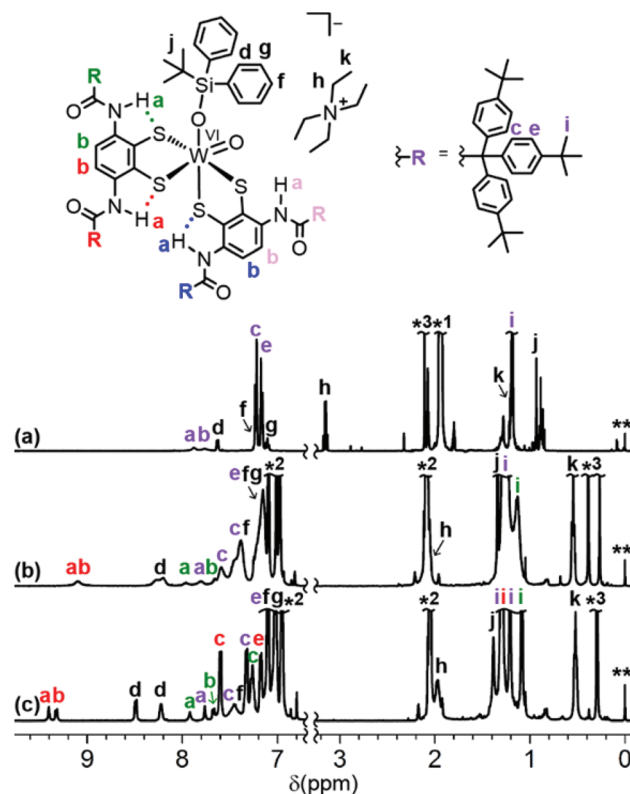


Fig. 2 ¹H NMR spectra of **3** in (a) CD₃CN at 30 °C, (b) toluene-*d*₈ at 30 °C, and (c) toluene-*d*₈ at –45 °C. The two set of assignable signals and unassignable signals are colored in red, green, and purple, respectively. The asterisks denote solvents (*1: acetonitrile; *2: toluene; *3: water). The double asterisk (**) denotes TMS.

the relatively weak *trans* influence of the siloxo ligand. The unassignable signals are shown in purple (Fig. 2). Interestingly, two distinct d protons were observed at 8.2 and 8.5 ppm (Fig. 2c), indicating that the two phenyl rings of the ^tBuPh₂SiO ligand in essentially nonequivalent environments can be distinguished owing to the slowing of the conformational change.

IR and resonance Raman spectra

The presence of NH...S hydrogen bonds was confirmed by IR spectroscopy. Amide NH stretching bands for **1** and **3** in the solid state are listed in Table 1, along with the values of related complexes **4** and **6**.²¹

The $\Delta\nu(\text{NH})$ values, the lower shifts of $\nu(\text{NH})$ than that of the corresponding compound without the NH...S hydrogen bond (RCONHPh), represent the strength of the hydrogen bond, as described in a previous paper.^{19,21}

The smaller $\Delta\nu(\text{NH})$ values of **1** (−57 cm^{−1}) and **3** (−26, −69 cm^{−1}) than those of **4** and **6** (−97 and −96 cm^{−1}, respectively) indicate the presence of weaker NH...S hydrogen bonds in the complexes with the siloxo ligand, which is consistent with the molecular structures in the crystal.

In monooxotungsten(vi) complex **3**, four $\nu(\text{NH})$ values are expected based on the molecular structure, but only two NH stretching bands (3377 and 3334 cm^{−1}) were observed. The NH bands of **3** were considered to be overlapped similar to related complex **6**, which exhibited a single band (3316 cm^{−1}) of two $\nu(\text{NH})$ values (3326 and 3306 cm^{−1} by curve-fitting simulation).²¹

Resonance Raman spectra of desoxomolybdenum(IV) complex **1** excited at 514.5 nm exhibited a single signal at 919 cm^{−1} (Fig. S3a†). In the IR spectrum of the related complex, (Et₄N)[Mo^{IV}(OSi^tBuPh₂)(bdt)₂] (**7**), the corresponding band at 947 cm^{−1} was assigned to $\nu(\text{O-Si})$.¹⁴ In the case of monooxotungsten(vi) complex **3**, strong (924 cm^{−1}) and weak (889 cm^{−1}) signals were observed (Fig. S3b†), whereas the corresponding signals of (Et₄N)[W^{IV}O(OSi^tBuPh₂)(bdt)₂] at 933 and 888 cm^{−1} were assigned to $\nu(\text{O-Si})$ and $\nu(\text{W=O})$ by IR, respectively.²² However, because the sample was excited at the LMCT absorption band, the signal of $\nu(\text{W=O})$ should be more intense than that of $\nu(\text{O-Si})$ owing to the resonance effect (Fig. S4†). In order to assign the vibrational mode of these complexes, we estimated the frequency by DFT calculations and compared them with the observed values in the resonance Raman measurements of reported complexes containing bdt ligands (Fig. S3c, d†).^{14,22} As illustrated in Fig. S3† the signal

Table 1 IR bands of $\nu(\text{NH})$ (cm^{−1}) in the molybdenum and tungsten complexes in the solid state

	Complexes ^a	$\Delta(\text{NH})^b$
1	3346	−57
3	3377, 3334	−26, −69
4 ^c	3306	−97
6 ^c	3316	−87

^a Nujol. ^b Differences from the value (3403 cm^{−1}) of the corresponding compound, RCONHPh, in solution (10 mM in CH₂Cl₂). ^c Ref. 21.

of the molybdenum(IV) complex was assigned to Mo–O stretching combined with O–Si stretching, and the signals of the tungsten(vi) complex were assigned to symmetric and asymmetric WO₂ stretchings combined with O–Si stretching. The bands of **1** and **3** involving the M–O bonds were observed at lower wavenumbers than those of the corresponding bdt complexes; however, it is difficult to evaluate the influence of NH...S hydrogen bonds on the M–O bonds because of the complicated coupling of the stretching bands, as described above.

Oxygen-atom-transfer reactions

The OAT reaction between Me₃NO and complex **1** was monitored using UV-vis spectroscopy. Upon adding 2 equiv. of Me₃NO in DMF to **1** in toluene, a fast reaction occurred to afford a dark green solution (Fig. 3). The UV-vis spectrum obtained after the OAT reaction (red solid line) was identical to that of **2** (red dotted line), which indicated the clear and quantitative conversion of **1** into **2**. The second-order rate constant, k_2 , of the reaction was calculated to be 98 M^{−1} s^{−1}.

In a polar toluene–acetonitrile solution (*v/v* = 1/1 with a dielectric constant (ϵ_r) of approximately 25²⁸), the reaction rate ($k_2 = 8.6 \text{ M}^{-1} \text{ s}^{-1}$) was about ten times smaller than that in toluene, which was consistent with the results of a previous study, suggesting that the approach of a polar substrate was more efficient in a hydrophobic environment.²¹

Notably, these k_2 values were smaller in both polar and nonpolar solvents than those of the OAT reaction between **4** and Me₃NO ($k_2 = 26.6$ and $384 \text{ M}^{-1} \text{ s}^{-1}$ in DMF ($\epsilon_r = 36.7$)²⁹ and toluene, respectively).²¹ This was ascribed to the steric hindrance of bulky CAR₃ moieties and the ^tBuPh₂SiO[−] ligand and/or the decrease of the ionicity of the active center by the replacement of the dianionic O^{2−} ligand with the monoanionic ^tBuPh₂SiO[−] ligand.

Unfortunately, the solubility of complex **1** in acetonitrile was not enough to determine the k_2 of the reaction. In another polar solvent (DMF), **1** was unstable and hence decomposed

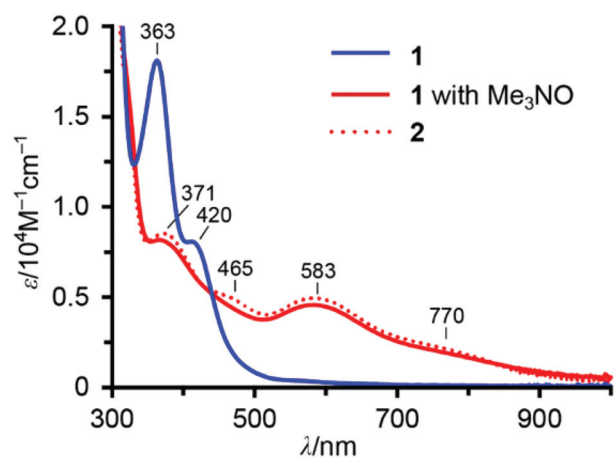


Fig. 3 UV-vis spectra of **1** (blue), the reaction mixture of **1** with 2 eq. of Me₃NO (red, solid), and *in situ* synthesized **2** by silylation of **5** (red, dotted) in toluene.

into **4** by the dissociation of the silyl group, and its reaction with Me_3NO afforded dioxomolybdenum(vi) complex **5**.

On the other hand, complex **1** was stable for several hours in an aqueous micellar solution containing Triton X-100, even in the presence of Me_3NO (Fig. S5[†]), indicating the formation of a robust hydrophobic microenvironment that prevents the approach of water molecules and polar substrates.

Addition of a large excess (400 eq.) of DMSO to **1** in toluene at 27 °C resulted in the oxidative dissociation of the dithiolate ligand to afford a disulfide derivative, L_{12} . These results suggest that a large excess of the coordinating compound with a large donor number (D_N)²⁹ tends to dissociate the ligands of **1**.

Surprisingly, complex **1** could reduce DMSO into Me_2S in toluene- d_8 , while no reaction occurred between monooxomolybdenum(iv) complex **4** and DMSO at 80 °C for 20 h. The reaction system containing 1.2 mM of **1** and 4.6 equiv. of DMSO in toluene- d_8 was monitored using ^1H NMR spectroscopy. No significant change in the spectrum was observed at r.t. for 24 h; however, heating the mixture at 50 °C resulted in the slow consumption of DMSO and **1**, accompanied by the production of Me_2S (Fig. 4, S6[†]). The reaction accomplished within 600 h, and the second-order kinetic constant estimated from the conversion of **1** was $k_2 = 5.7 \times 10^{-4} \text{ M}^{-1} \text{ s}^{-1}$ (Fig. S7a[†]). Accompanied by the decrease in the signals of **1**, neither the signals of amide NH nor the benzenedithiolate protons of the product were observed, whereas a broad signal of ^tBu protons in the CAr_3 moiety was observed. The result suggests the formation of paramagnetic species. After the complete consumption of **1**, the UV-vis spectrum of the reaction mixture showed the absorption band at 756 nm (Fig. S8[†]), which is characteristic of five-coordinated monooxomolybdenum(v) complexes.^{30–32} One-electron oxidation of **4** by 1.1 equiv. of $[\text{Fe}^{\text{III}}\text{Cp}_2]\text{BF}_4$ proceeded quickly and quantitatively in toluene to afford the monooxomolybdenum(v) complex, $(\text{Et}_4\text{N})[\text{Mo}^{\text{V}}\text{O}(\text{1,2-S}_2\text{-3,6-}\{(4\text{-}^t\text{BuC}_6\text{H}_4)_3\text{CCONH}\}_2\text{C}_6\text{H}_2)_2]$. By comparing the absorbance at 756 nm, the yield of the Mo(v) species was found to be approximately 70%. Moreover, sharp signals of $^t\text{BuPh}_2\text{SiOH}$ were observed. The result is similar to that observed for monooxomolybdenum(vi) complex, **8**, which decomposes by a homolytic cleavage of the $\text{Mo}^{\text{VI}}\text{-OPh}$ bond to

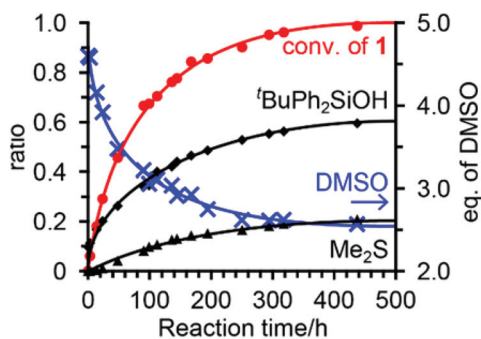
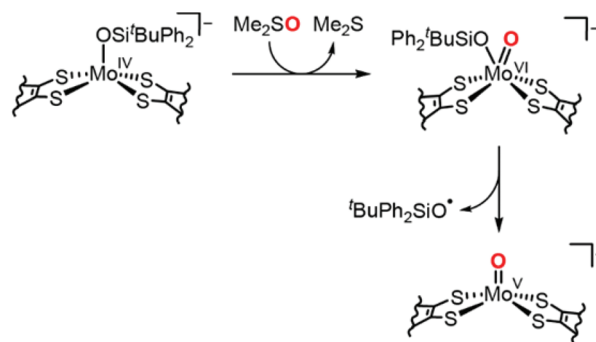


Fig. 4 Time course of the conversion of **1** during the reduction of DMSO in toluene- d_8 .



Scheme 2 The proposed mechanism of the OAT reaction of DMSO.

afford the corresponding monooxomolybdenum(v) complex and phenol.^{16,33} The dissociative mechanism is consistent with the ~60% production of $^t\text{BuPh}_2\text{SiOH}$ (Scheme 2). In addition, 2 equiv. of DMSO was consumed while ~20% of Me_2S based on the initial amount of **1** was detected, probably owing to the decomposition of the product through a radical process.

A similar OAT reaction occurred in a mixture of toluene- d_8 and acetonitrile- d_3 ($v/v = 1/1$, Fig. S7[†]). The similar reaction rate ($k_2 = 6.7 \times 10^{-4} \text{ M}^{-1} \text{ s}^{-1}$) to that in toluene- d_8 indicates that the desoxomolybdenum(iv) complex can reduce DMSO without depending on the solvent polarity, unlike the case of Me_3NO . The polar amine *N*-oxide is hardly soluble in nonpolar solvents and considered to be condensed into the ionic active center. Thus, the dramatic acceleration of the OAT reaction was achieved, as described in a previous paper.²¹ In contrast, DMSO can diffuse uniformly even in toluene, and only the hydrophobic microenvironment around the active center affects the uptake of the substrate. Similar reactivity in both polar and nonpolar solvents indicates the presence of a hydrophobic microenvironment for efficient uptake of the substrate.

Discussion

Desoxomolybdenum(iv) complex **1** containing bulky hydrophobic substituents could reduce DMSO in both polar and nonpolar solvents. Although it is difficult to quantitatively discuss the reaction because of the instability of the resulting monooxomolybdenum(vi) complex **2** under the reaction conditions, the production of Me_2S was confirmed by ^1H NMR analysis. Moreover, the clean and quantitative OAT reaction of **1** with Me_3NO was also observed.

In the case of the siloxomolybdenum(iv) complex containing unsubstituted bdt ligands (**7**), no appreciable reaction was observed when a large excess of more reactive tetramethylene sulfoxide ($(\text{CH}_2)_4\text{SO}$) was reacted in CH_3CN on heating at 50 °C, whereas the OAT reaction of Me_3NO occurred, but it was not clean.¹⁴ Phenoxomolybdenum(iv) complex **8** slowly reacted with a large excess of DMSO in CH_3CN on heating, and the kinetic parameters ΔH^\ddagger and ΔS^\ddagger were reported to be 14.8(5) kcal mol⁻¹ and -36(1) cal mol⁻¹, respectively.^{16,33} The esti-

mated k_2 at 50 °C from the Eyring plot was $8 \times 10^{-6} \text{ M}^{-1} \text{ s}^{-1}$, which was much smaller than the present system. In another case, a siloxomolybdenum(IV) complex, $(\text{Et}_4\text{N})[\text{Mo}^{\text{IV}}(\text{OSi}^i\text{BuPh}_2)\text{-}\{\text{S}_2\text{C}_2(\text{COOCH}_3)_2\}_2]$, was reported to cleanly react with Me_3NO below -15 °C; however, the reaction with DMSO was too slow to be monitored.¹² In addition, a monooxomolybdenum(IV) complex containing 4,5-dimethoxy-1,2-benzenedithiolate ligands was reported to catalyze the reduction of DMSO by Ph_3P ; however, a large excess of DMSO as a solvent was used.¹³

The enhanced reactivity of the desoxomolybdenum(IV) complex in the present system is considered to be caused by the stabilization of the DMSO-bound transient structure owing to bulky hydrophobic substituents. The DFT calculations of desoxomolybdenum(IV) complexes indicated that the distortion of the geometry and trigonal-prismatic transition state are important to promote the attack of DMSO *cis* to the alkoxo ligand.¹⁷ In our theoretical investigation of monooxomolybdenum(IV) complexes, we have shown that the four bulky ligands stabilize the transient distorted structure and promote the very fast OAT reaction of Me_3NO through a direct *cis*-attack mechanism.¹⁹

Furthermore, the hydrophobic microenvironment around the active center is found to be maintained regardless of the solvent polarity. These results indicate that desoxomolybdenum(IV) complex **1** ensures the substrate-access pocket for DMSO.

Conclusions

Toluene-soluble desoxomolybdenum(IV), monooxomolybdenum(VI), and monooxotungsten(VI) complexes (**1–3**, respectively) containing bulky hydrophobic groups were synthesized. The simple modification of an oxo ligand into a siloxo ligand achieved the reduction of not only Me_3NO but also DMSO. Moreover, the reduction of DMSO was accelerated compared to that of the other complexes.

The rate of the OAT reaction of DMSO was independent of the polarity of the reaction media, which suggests the formation of a hydrophobic microenvironment around the active center. The combination of the bulkiness of CAr_3 groups and a hydrophobic microenvironment promoted the OAT reaction of the biological substituent, DMSO, by forming the confined space for substrate binding.

Acknowledgements

This work was supported by JSPS KAKENHI Grant Number 26410072.

Notes and references

1 R. Hille, J. Hall and P. Basu, *Chem. Rev.*, 2014, **114**, 3963–4038.

- 2 H. Schindelin, C. Kisker, J. Hilton, K. V. Rajagopalan and D. C. Rees, *Science*, 1996, **272**, 1615–1621.
- 3 N. Cobb, C. Hemann, G. A. Polsinelli, J. P. Ridge, A. G. McEwan and R. Hille, *J. Biol. Chem.*, 2007, **282**, 35519–35529.
- 4 K. E. Johnson and K. V. Rajagopalan, *J. Biol. Chem.*, 2001, **276**, 13178–13185.
- 5 A. S. McAlpine, A. G. McEwan and S. Bailey, *J. Mol. Biol.*, 1998, **275**, 613–623.
- 6 S. Mondal and P. Basu, *Inorg. Chem.*, 2001, **40**, 192–193.
- 7 R. H. Holm, E. I. Solomon, A. Majumdar and A. Tenderholt, *Coord. Chem. Rev.*, 2011, **255**, 993–1015.
- 8 F. J. Hine, A. J. Taylor and C. D. Garner, *Coord. Chem. Rev.*, 2010, **254**, 1570–1579.
- 9 V. W. L. Ng, M. K. Taylor and C. G. Young, *Inorg. Chem.*, 2012, **51**, 3202–3211.
- 10 P. Basu and S. J. N. Burgmayer, *Coord. Chem. Rev.*, 2011, **255**, 1016–1038.
- 11 H. Sugimoto, S. Tatemoto, K. Suyama, H. Miyake, R. P. Mtei, S. Itoh and M. L. Kirk, *Inorg. Chem.*, 2010, **49**, 5368–5370.
- 12 A. Majumdar and S. Sarkar, *Coord. Chem. Rev.*, 2011, **255**, 1039–1054.
- 13 A. Döring, C. Fischer and C. Schulzke, *Z. Anorg. Allg. Chem.*, 2013, **639**, 1552–1558.
- 14 J. P. Donahue, C. R. Goldsmith, U. Nadiminti and R. H. Holm, *J. Am. Chem. Soc.*, 1998, **120**, 12869–12881.
- 15 B. S. Lim, J. P. Donahue and R. H. Holm, *Inorg. Chem.*, 2000, **39**, 263–273.
- 16 B. S. Lim and R. H. Holm, *J. Am. Chem. Soc.*, 2001, **123**, 1920–1930.
- 17 Y. Ha, A. L. Tenderholt, R. H. Holm, B. Hedman, K. O. Hodgson and E. I. Solomon, *J. Am. Chem. Soc.*, 2014, **136**, 9094–9105.
- 18 K. Baba, T. Okamura, C. Suzuki, H. Yamamoto, T. Yamamoto, M. Ohama and N. Ueyama, *Inorg. Chem.*, 2006, **45**, 894–901.
- 19 T. Okamura, Y. Ushijima, Y. Omi and K. Onitsuka, *Inorg. Chem.*, 2013, **52**, 381–394.
- 20 K. Baba, T. Okamura, H. Yamamoto, T. Yamamoto, M. Ohama and N. Ueyama, *Chem. Lett.*, 2005, **34**, 44–45.
- 21 Y. Hasenaka, T. Okamura, M. Tatsumi, N. Inazumi and K. Onitsuka, *Dalton Trans.*, 2014, **43**, 15491–15502.
- 22 C. Lorber, J. P. Donahue, C. A. Goddard, E. Nordlander and R. H. Holm, *J. Am. Chem. Soc.*, 1998, **120**, 8102–8112.
- 23 A. Altomare, G. Cascarano, C. Giacovazzo and A. Guagliardi, *J. Appl. Crystallogr.*, 1994, **27**, 435–436.
- 24 P. T. Beurskens, G. Admiraal, H. Behm, G. Beurskens, J. M. M. Smits and C. Smykalla, *Z. Kristallogr.*, 1991 (Suppl. 4), 99.
- 25 G. M. Sheldrick, *Acta Crystallogr., Sect. A: Fundam. Crystallogr.*, 2008, **64**, 112–122.
- 26 M. J. Frisch, G. W. Trucks, H. B. Schlegel, G. E. Scuseria, M. A. Robb, J. R. Cheeseman, J. A. Montgomery, Jr.,

- T. Vreven, K. N. Kudin, J. C. Burant, J. M. Millam, S. S. Iyengar, J. Tomasi, V. Barone, B. Mennucci, M. Cossi, G. Scalmani, N. Rega, G. A. Petersson, H. Nakatsuji, M. Hada, M. Ehara, K. Toyota, R. Fukuda, J. Hasegawa, M. Ishida, T. Nakajima, Y. Honda, O. Kitao, H. Nakai, M. Klene, X. Li, J. E. Knox, H. P. Hratchian, J. B. Cross, V. Bakken, C. Adamo, J. Jaramillo, R. Gomperts, R. E. Stratmann, O. Yazyev, A. J. Austin, R. Cammi, C. Pomelli, J. W. Ochterski, P. Y. Ayala, K. Morokuma, G. A. Voth, P. Salvador, J. J. Dannenberg, V. G. Zakrzewski, S. Dapprich, A. D. Daniels, M. C. Strain, O. Farkas, D. K. Malick, A. D. Rabuck, K. Raghavachari, J. B. Foresman, J. V. Ortiz, Q. Cui, A. G. Baboul, S. Clifford, J. Cioslowski, B. B. Stefanov, G. Liu, A. Liashenko, P. Piskorz, I. Komaromi, R. L. Martin, D. J. Fox, T. Keith, M. A. Al-Laham, C. Y. Peng, A. Nanayakkara, M. Challacombe, P. M. W. Gill, B. Johnson, W. Chen, M. W. Wong, C. Gonzalez and J. A. Pople, *GAUSSIAN 03 (Revision E.01)*, Gaussian, Inc., Wallingford CT, 2004.
- 27 N. Ueyama, T. Okamura and A. Nakamura, *J. Am. Chem. Soc.*, 1992, **114**, 8129–8137.
- 28 G. Ritzoulis, N. Papadopoulos and D. Jannakoudakis, *J. Chem. Eng. Data*, 1986, **31**, 146–148.
- 29 J. A. Riddick, W. B. Bunger and T. K. Sakano, *Organic Solvents: Physical Properties and Methods of Purification*, Wiley, New York, 1986.
- 30 S. Boyde, S. R. Ellis, C. D. Garner and W. Clegg, *J. Chem. Soc., Chem. Commun.*, 1986, 1541–1543.
- 31 R. L. McNaughton, M. E. Helton, N. D. Rubie and M. L. Kirk, *Inorg. Chem.*, 2000, **39**, 4386–4387.
- 32 N. Ueyama, N. Yoshinaga, T. Okamura, H. Zaima and A. Nakamura, *J. Mol. Catal.*, 1991, **64**, 247–256.
- 33 B. S. Lim, K.-M. Sung and R. H. Holm, *J. Am. Chem. Soc.*, 2000, **122**, 7410–7411.

Copyright of Dalton Transactions: An International Journal of Inorganic Chemistry is the property of Royal Society of Chemistry and its content may not be copied or emailed to multiple sites or posted to a listserv without the copyright holder's express written permission. However, users may print, download, or email articles for individual use.